Synthetic receptors as models for alkali metal cation-π binding sites in proteins

Stephen L. De Wall[†], Eric S. Meadows[†], Leonard J. Barbour[‡], and George W. Gokel[†§]

[†]Bioorganic Chemistry Program and Department of Molecular Biology and Pharmacology, Washington University School of Medicine, 660 South Euclid Avenue, Campus Box 8103, St. Louis, MO 63110; and [‡]Department of Chemistry, University of Missouri, 601 South College Avenue, Columbia, MO 65211

Communicated by Kenneth N. Raymond, University of California, Berkeley, CA, March 22, 2000 (received for review December 7, 1999)

The alkali metal cations Na^+ and K^+ have several important physiological roles, including modulating enzyme activity. Recent work has suggested that alkali metal cations may be coordinated by π systems, such as the aromatic amino acid side chains. The ability of K^+ to interact with an aromatic ring has been assessed by preparing a family of synthetic receptors that incorporate the aromatic side chains of phenylalanine, tyrosine, and tryptophan. These receptors are constructed around a diaza-18-crown-6 scaffold, which serves as the primary binding site for an alkali metal cation. The ability of the aromatic rings to coordinate a cation was determined by crystallizing each of the receptors in the presence of K^+ and by solving the solid state structures. In all cases, complexation of K^+ by the π system was observed. When possible, the structures of the unbound receptors also were determined for comparison. Further proof that the aromatic ring makes an energetically favorable interaction with the cation was obtained by preparing a receptor in which the arene was perfluorinated. Fluorination of the arene reverses the electrostatics, but the aromaticity is maintained. The fluorinated arene rings do not coordinate the cation in the solid state structure of the K^+ complex. Thus, the results of the predicted electrostatic reversal were confirmed. Finally, the biological implications of the alkali metal cation-π interaction are addressed.

It has been known for more than 30 years that the presence or absence of the alkali metal cations Na^+ and K^+ may dramatically affect the activity of certain enzymes (1). Until recently, however, the chemical mechanism by which these cations acted was unknown. In several proteins, binding sites for Na^+ and K^+ have been identified by x-ray crystallographic analyses (2, 3). The alkali metal binding sites in such proteins seem to serve two purposes. The bound cation may play a structural role, in which case it is not located at the chemically reactive site (4, 5). The cation or cations are proposed to stabilize a particular conformation of the protein in this situation. In a second group of proteins, the alkali metal cation(s) is located at the active site (6–8). It is thought that in this case, alkali metals are present to maintain a charge balance during the catalytic process.

The solid state structures of these proteins show alkali metal cations are typically bound by polar, σ donor groups such as carbonyl, hydroxyl, carboxylate, and water (9). The oxygen(s) in these functional groups serves as the coordinating heteroatom. However, evidence from calculations (10–12), gas phase studies (13–15), and small-molecule crystal structures (16–18) indicates that aromatic groups, traditionally thought to be "hydrophobic" or "nonpolar," may also be able to bind either Na^+ or K^+ (19). The three aromatic amino acids that might serve as π donors for an alkali metal cation are Phe, Trp, and Tyr. The side chains of aromatic residues have been observed coordinating Cs^+, a large alkali metal cation, in crystal structures of rhodanese (20), glutamine synthetase (21), and methylamine dehydrogenase (22). In a recently reported crystal structure of lysozyme (PDB ID code 1LPI), a Na^+ cation is observed to interact with a solvent-exposed Trp side chain (23). There is also strong structural evidence that Mg^{2+} interacts directly with the π face of the bases in DNA and RNA (24).

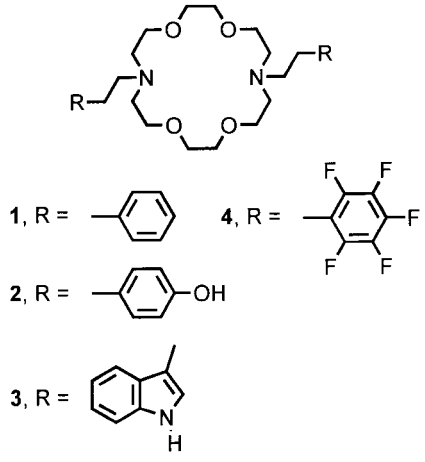

Scheme 1.

Evidence for alkali metal cation-π interactions in biological systems is sparse and currently limited to the examples in the proteins listed above. However, the ability of ammonium cations to interact with aromatic amino acids has been observed in many cases (25). There is now sufficient evidence that the ammonium cation-π interaction can be considered an important noncovalent force in protein stabilization (26, 27) and molecular recognition (19, 25). We suggest that alkali metal cation-π interactions may simply not be as well documented and consequently not appreciated. To obtain "high-resolution" data for alkali metal cation-π interactions, we have prepared and studied a family of synthetic receptors. These receptors were designed to incorporate the aromatic side chains of Phe (benzene), Trp (indole), and Tyr (phenol).

The structures of the receptors having benzene (compound **1**), phenol (compound **2**), and indole (compound **3**) sidearms, corresponding to the aromatic amino acids, are shown (see Scheme 1). The design of the receptors is based on the diaza-18-crown-6 scaffold. Sidearms may be attached at the nitrogen atoms on opposite sides of the macroring. The ability of nitrogen to readily invert confers an overall flexibility on the system. Cation binding was envisioned to occur by macroring complexation of the cation followed by apical coordination by the arene-substituted sidearms. Such a binding mode is well known for the two-armed (bibracchial) lariat ether compounds (28). The 18-membered ring size was chosen because of the macroring's overall symmetry and its size correspondence with the K^+ cation.

Abbreviation: CSD, Cambridge Structural Database.

[§]To whom reprint requests should be addressed. E-mail: ggokel@molecool.wustl.edu.

The publication costs of this article were defrayed in part by page charge payment. This article must therefore be hereby marked "*advertisement*" in accordance with 18 U.S.C. §1734 solely to indicate this fact.

The ethylene spacer was selected based on an analysis with Corey-Pauling-Koltun molecular models. The two-carbon spacer between macroring nitrogen and the arene is appropriate to achieve the apical cation-π interaction sought and also is the number of carbons between nitrogen and the arene in the natural amino acids.

We have recently reported compounds **2** and **3**, which incorporate the electron-rich π systems phenol and indole, respectively (29, 30). In both receptors, K^+ was bound as a π sandwich complex. We now report the successful π complexation of K^+ using a receptor, **1**, having sidearms corresponding to the phenylalanine sidechain. We compare the cation-π interactions observed for receptors **1**, **2**, and **3**. In addition, we have prepared compound **4**, a fluorinated analog of **1**, to determine the effect that reversing the electrostatics of the aromatic ring has on π complexation. Synthetic receptors **1**, **2**, **3**, and **4** were prepared and crystallized in the absence and presence of K^+ cation. Solid state structures were then determined by x-ray crystallography.

Materials and Methods

General. ^{1}H NMRs were recorded at 300 MHz in $CDCl_3$ and are reported in ppm (δ, Me_4Si). Melting points were determined on a Thomas Hoover apparatus in open capillaries and are uncorrected. All reactions were conducted under dry N_2 unless otherwise stated. All reagents were the best (non-liquid chromatography) grade commercially available and were used without further purification. Combustion analyses were performed by Atlantic Microlab (Atlanta, GA) and are reported as percentages.

***N,N′*-bis(2-phenylethyl)-4,13-diaza-18-crown-6,1.** A solution of (2-bromoethyl)benzene (0.727 g, 3.93 mmol), 4,13-diaza-18-crown-6 (0.515 g, 1.96 mmol), and Na_2CO_3 (0.519 g, 4.9 mmol) was stirred in refluxing acetonitrile (20 ml) for 24 h. The crude product was cooled to room temperature, filtered, concentrated *in vacuo*, dissolved in CH_2Cl_2 (100 ml), washed three times with H_2O (15 ml), and the organic phase was dried over $MgSO_4$, filtered, and concentrated again *in vacuo* to afford a yellow oil. The oil was purified by flash column chromatography [silica, 5% Et_3N in acetone (vol/vol)] to give the desired product as a colorless oil. After 24 h under high vacuum, the oil solidified (0.554 g, 60% yield): mp 48–50°C; ^{1}H NMR 2.77 (s, crown—CH_2CH_2—phenyl, 8H), 2.86 (t, —NCH_2CH$_2$—, 8H), 3.62 (m, —CH_2OCH_2—, 16H), 7.15–7.30 (m, phenyl, 10H). Analysis calculated for $C_{28}H_{42}N_2O_4$: C, 71.46; H, 8.99; N, 5.95. Found: C, 71.20; H, 9.00; N, 5.90.

***N,N′*-bis(2-(4-hydroxyphenyl)ethyl)-4,13-diaza-18-crown-6,2.** This compound was prepared as previously described (29).

***N,N′*-bis(2-(3-indolyl)ethyl)-4,13-diaza-18-crown-6,3.** This compound was prepared as previously described (30).

***N,N′*-bis[2-(2,3,4,5,6-pentafluorophenyl)ethyl]-4,13-diaza-18-crown-6,4.** *2,3,4,5,6-Pentafluorophenylacetyl chloride.* A solution of 2,3,4,5,6-pentafluorophenylacetic acid (1.0 g, 4.42 mmol) was stirred in CH_2Cl_2 (50 ml) in an ice bath. Next, a 2.0 M solution of oxalyl chloride in CH_2Cl_2 (2.21 ml, 4.42 mmol) was added dropwise, and a catalytic amount of anhydrous dimethylformamide then was added to the reaction flask. The reaction mixture was removed from the ice bath and stirred at ambient temperature for 1 h. The CH_2Cl_2 was removed *in vacuo* to give the desired acid chloride as a solid that was stored under N_2 and used in the next step without further purification.

N,N′-bis[2-(2,3,4,5,6-pentafluorophenyl)ethylamide]-4,13-diaza-18-crown-6. A solution of 4,13-diaza-18-crown-6 (0.580 g, 2.21 mmol) and Et_3N (0.62 ml, 4.42 mmol) in CH_2Cl_2 (20 ml) was cooled in an ice bath. An ice-cold solution of 2,3,4,5,6-pentafluorophenylacetyl chloride (1.08 g, 4.42 mmol) in CH_2Cl_2 (20 ml) was added dropwise. After addition of the acid chloride, the ice bath was removed and stirring was continued for 24 h at ambient temperature. The reaction mixture was filtered and concentrated *in vacuo* to give an orange oil. Crystallization from EtOAc gave the desired amide as a white solid (1.04 g, 70%): mp 132°C.

N,N′-bis[2-(2,3,4,5,6-pentafluorophenyl)ethyl]-4,13-diaza-18-crown-6. The bis(amide) compound (see above, 0.150 g, 0.221 mmol) was dissolved in tetrahydrofuran (10 ml) at 0°C. A solution of BH_3·tetrahydrofuran (1 M, 10 ml) then was added, the ice bath was removed, and the mixture was stirred for 24 h at ambient temperature. The reaction mixture was concentrated *in vacuo*, HCl (6 M, 10 ml) was added, and the solution was heated at reflux for 30 min. The solution was cooled to 0°C and made basic by adding NaOH pellets. The basic solution was extracted with EtOAc, and the organic phase was dried over anhydrous $MgSO_4$, filtered, and concentrated *in vacuo*. The desired product was isolated without further purification as a white solid (0.124 g, 86%): mp 61–62°C; 1H NMR 2.73–2.86 (m, —CH_2NCH_2CH_2—perfluorophenyl, 16H), 3.56 (t, —NCH$_2$ CH_2O—, 8H), 3.58 (s, —OCH_2CH_2O—, 8H). Analysis calculated for $C_{28}H_{32}F_{10}N_2O_4$: C, 51.69; H, 4.96; N, 4.31. Found: C, 51.50; H, 5.04; N, 4.19.

Crystallization of 1·KI. Equivalent amounts of **1** and KI were mixed in EtOAc at ambient temperature. Slow evaporation of the solvent during several weeks afforded the complex as colorless crystals.

Crystallization of 4 and 4·KI. A nearly saturated ethyl acetate solution was prepared of **4**. Slow evaporation during several weeks gave crystals of **4** that were suitable for x-ray analysis. Equivalent amounts of **4** and KI were mixed in Me_2CO at ambient temperature. Slow evaporation of the solvent during several weeks afforded **4**·KI as colorless crystals.

X-Ray Crystallography. Intensity data for all crystals reported here were collected at 173(1) K on a Bruker (Billerica, MA) SMART charge-coupled device diffractometer (ω scan mode Mo-K_α radiation, $\lambda = 0.7107$ Å). Data were corrected for absorption by using the program SADABS (31). Structure solution and refinement proceeded similarly for all structures [SHELX-97 software (obtained from G. M. Sheldrick, University of Göttingen, Germany) using the X-SEED (http://www.lbarbour.com/xseed/). interface]. Direct methods yielded all nonhydrogen atoms of the asymmetric unit. These atoms were refined anisotropically (full-matrix least-squares method on F^2). Hydrogen atoms were placed in calculated positions with their isotropic thermal parameters riding on those of their parent atoms. Fig. 1 was prepared with X-SEED and POV-RAY (http://www.povray.org).

Crystal Data for 1·KI. $M = 636.64$; colorless rhombohedroids, $0.40 \times 0.30 \times 0.15$ mm^3; monoclinic, C 2/c; a = 19.9098(9) Å, b = 9.6181(4) Å, c = 17.2441(8) Å, $\beta = 116.4390(10)°$; $Z = 4$; $V = 2956.8(2)$ Å^3; $D_c = 1.430$ g/mm^3; $2\theta_{max} = 54.24°$, 8,740 reflections collected and 3,248 unique [R(int) = 0.0185]; final *GoF* = 1.046, *R1* = 0.0231, *w*R2 = 0.0594, *R* indices based on 2,982 reflections with $I > 2\sigma(I)$, $\mu = 1.258$ mm^{-1}, minimum transmission factor = 0.6331.

Crystal Data for 4. $M = 650.56$; colorless rhombohedroids, $0.25 \times 0.25 \times 0.10$ mm^3; monoclinic, P 21/c; a = 15.0714(17) Å, b = 9.5904(11) Å, c = 9.9806(11) Å, $\beta = 95.185(2)°$; $Z = 2$; $V = 1436.7(3)$ Å^3; $D_c = 1.504$ g/mm (3); $2\theta_{max} = 54.22°$, 8,742 reflections collected and 3,162 unique [R(int) = 0.0392]; final *GoF* = 0.887, *R1* = 0.0406, *w*R2 = 0.0871, *R* indices based on

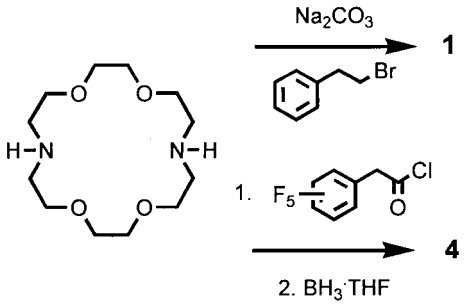

Scheme 2.

1,821 reflections with $I > 2\sigma(I)$, $\mu = 0.143$ mm^{-1}, minimum transmission factor = 0.9652.

Crystal Data for 4·KI. $M = 816.56$; colorless rhombohedroids, $0.25 \times 0.25 \times 0.20$ mm^3; triclinic, P -1; a = 8.0839(6) Å, b = 8.2103(6) Å, c = 13.9553(11) Å, $\alpha = 97.9020(10)°$, $\beta = 97.2120(10)°$; $\gamma = 115.0700(10)°$. $Z = 1$; $V = 813.38(11)$ Å^3; $D_c = 1.667$ g/mm^3; $2\theta_{max} = 54.22°$, 5,052 reflections collected and 3,482 unique [R(int) = 0.0207]; final *GoF* = 1.041, *R1* = 0.0526, *w*R2 = 0.1311, *R* indices based on 3,042 reflections with $I > 2\sigma(I)$, $\mu = 1.206$ mm^{-1}, minimum transmission factor = 0.7526.

Cambridge Structural Database (CSD) Search. Version 5.17 of the CSD, containing over 190,000 entries of small-molecule crystal structures, was analyzed with the QUEST 3-D browser. The input fragment consisted of a secondary amide and one of the following: a water molecule, Na^+, or K^+ (Z···O = C, where Z = O_{water}, Na^+, or K^+). The maximum for an accepted interaction between Z and the carbonyl oxygen (Z···O) was set to 4 Å, and the Z···O = C angle was set from 0° to 180°. Only well determined ($R < 10\%$) and error-free structures were considered. The search criteria resulted in 338, 34, and 36 structures that matched the results of the amide-water, amide-Na^+, and amide-K^+ complexes, respectively.

Results and Discussion

Preparation of Receptors. The phenylethyl (**1**)- and indolylethyl (**3**)-sidearmed compounds were prepared by alkylation of diaza-18-crown-6 with 2-bromoethylbenzene or 3-(2-bromoethyl)indole, respectively. Phenol-sidearmed **2** was prepared by cyclizing tyramine and 1,2-bis(2-iodoethoxy)ethane in the presence of Na_2CO_3 (32). Finally, compound **4** was prepared by acylation of diaza-18-crown-6 with 2,3,4,5,6-pentafluorophenylacetyl chloride followed by reduction with BH_3·tetrahydrofuran (see Scheme 2).

Solid State Structure of 1. The formation of the KI complex of **1** is shown in semischematic form in Fig. 1*a*. Unbound **1** is a low-melting solid (mp 48–50°C), and we have not obtained crystals suitable for x-ray analysis. The conformation of the unbound compound therefore is illustrated based on the conformation of the other unbound receptors in this family, **2** and **3**, which have been determined by x-ray crystallography (29, 30). The unbound structure of **4** also has been determined, and the macroring conformation is essentially identical to that observed for **2** and **3** (Fig. 1*d*).

The conformation of receptor **1** changes dramatically upon binding K^+. The solid state structure is shown (tube metaphor) in Fig. 1*a*, and a space-filling view is shown in Fig. 1*e* (*Top*). The x-ray analysis reveals that the macrocyclic ring is in the typical D_{3d} conformation. The four oxygen atoms are about equidistant from K^+ (2.68 ± 0.05 Å). Both K^+—N distances are longer than the K^+—O distances and both are identical: 3.06 Å. The ethylene sidearms are in the *gauche* conformation and reach above and below the mean plane of the crown. Each benzene ring occupies an apical position above and below the macroring forming a π sandwich complex with K^+. The "centerline" distance between the two centroids is 6.86 Å. The K^+ ion is 3.43 Å from the center of the aromatic ring.

The thickness of an arene is in the range 3.4–3.6 Å. By using a value of 3.5 Å as we have in previous work (29, 30), we conclude that the separation of opposite π surfaces in this complex is 3.36 Å. An octacoordinate K^+ ion has a diameter of 3.02 Å (33). Considering these values, a K^+ ion in van der Waals contact with an arene should exhibit a K^+–π distance of 3.26 Å, differing from the observed value (3.43 Å) by <0.2 Å on either side. We thus consider the cation to be complexed by the π surface of the arene.

An interesting comparison of **1**·KI can be made with the previously reported structure of the KSCN complex of *N*,*N*′-dibenzyl-4,13-diaza-18-crown-6 (34). This compound is identical to **1** except that the sidearms are phenylmethyl (benzyl) rather than phenylethyl. No sidearm participation is apparent in the K^+ complex of *N*,*N*′-dibenzyldiaza-18-crown-6, an observation in accord with Corey-Pauling-Koltun model structures: The benzyl sidearms are too short for intramolecular π complexation to occur.

Comparison of the Structures of 1–3. Cutaway views of the solid state structures of compounds **1**-**3** are shown in Fig. 1*b*. These receptors have in common the 4,13-diaza-18-crown-6 macroring and arene-terminated two-carbon side chains. The sidearms of **1** and **2** correspond to the side chains of phenylalanine and tyrosine. Compounds **1** and **2** are identical except for the hydroxyl group present at the terminus of each sidearm in the latter. The K^+ is positioned essentially in the center of the macroring in both **1**·KI and **2**·KI. In each case, the macrocycle adopts the D_{3d} conformation, and the K^+—O (2.68–2.70 Å) and K^+—N distances (3.04–3.06 Å) are essentially identical. The arene-arene separation is 6.86 Å in **1** and 6.88 Å in **2**. The most critical feature of both structures is the orientation of the arenes with respect to the ring-bound cation. The K^+ to arene centroid distances are 3.43 Å and 3.44 Å, respectively. The position of K^+ with respect to the aromatic ring's surface is nearly identical in **1** and **2** (Fig. 1*b*). In both cases, K^+ is essentially in the center of the benzene ring, and the arenes are parallel to each other (see Fig. 1*b*).

A significant difference concerns the position of the iodide counterion (shown in Fig. 1*b* as a magenta sphere). In **2**, each terminal hydroxyl group forms a hydrogen bond to iodide, positioning the latter essentially coplanar with one of the arenes and at a distance (O···I) of 3.47 Å. The O—H···I hydrogen bond angle is 170.5°. The KI complex of **1** lacks any hydroxyl group, and the iodide anion is positioned approximately coplanar with the cation and macroring. Two short C—H···I contacts (D = 4.26 and 4.16 Å, $\theta = 152.9°$ and 155.7°, respectively) are apparent in the structure of **1**·KI.

Solid state structures of **3**·KI and **3**·KPF_6 have been obtained. In both cases, the K^+ complexes exhibit similar receptor conformations. Irrespective of anion, the K^+ cation is aligned with the pyrrolo subunit of the indole sidearm at a nearly identical distance (3.45–3.48 Å). The two indolyl residues are parallel but the K^+ cation is closest to C-2 in the pyrrolo (five-membered ring) subunit (K^+—C2 = 3.30, 3.32 Å). In addition to the two K^+ structures, a Na^+-bound structure of **3** also has been determined (30). This structure is similar to the K^+ structures including the observed coordination of the cation by the pyrrolo subunit of indole.

Changing the π Donicity: Comparison of the Solid State Structures of 1 and 4. Compounds **1** and **4** are identical except that the aromatic rings of the latter are perfluorinated. Although the van der Waals radii of H (1.2 Å) and F (1.35 Å) differ slightly, the two

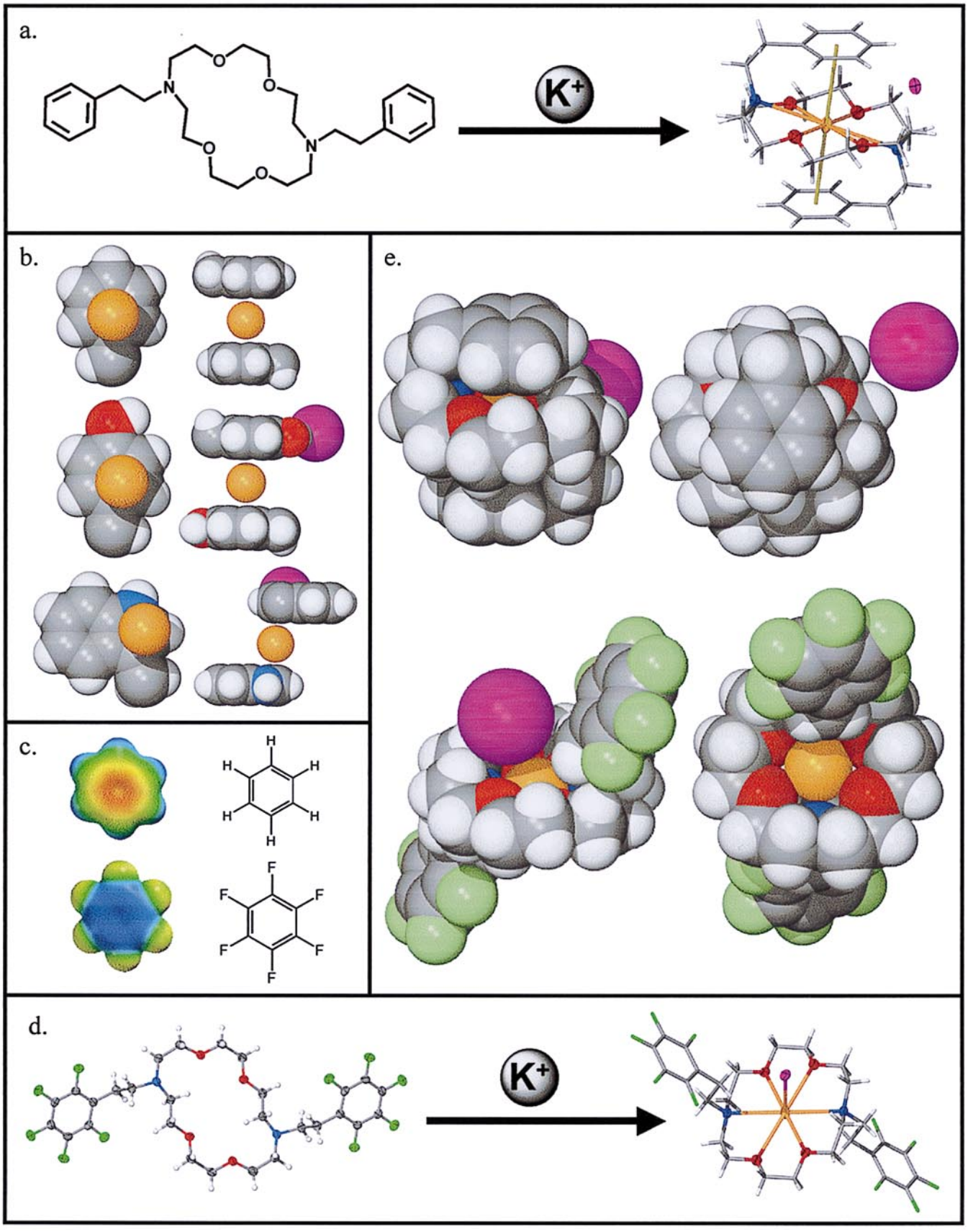

Fig. 1. (*a*) Complexation of K^+ by **1**. The depiction on the right is from the x-ray crystal structure. (*b*) Cation-π complexes observed in the solid state structures of **1**-**3**. (*c*) Electrostatic potential surface for benzene (*Top*) and hexafluorobenzene (*Bottom*). (*d*) Complexation of K^+ by **4**. (*e*) Comparison of the solid state structures of **1**·KI (*Top*) and **4**·KI (*Bottom*).

receptors are essentially isosteres. Compound **4** differs dramatically, however, in its π donicity, as compared with **1**. This difference is apparent from a comparison of the calculated electrostatic potential surfaces (10) (HF/6–31G**, PC Spartan Pro; Wavefunction, Irvine, CA) (Fig. 1*c*). The electrostatic potential surfaces are calculated for the arenes rather than for their substituted forms, but the difference is obvious. The cation-attracting negative potential in benzene (Fig. 1*c*) is at or near the arene's center (red, negative; blue, positive). In contrast, the perfluorinated benzene, although still fully aromatic, has a substantial positive potential at the center (indicated by the blue color).

The solid state structure of **4** was determined. The structure of the unbound receptor is shown in Fig. 1*d*. As noted above, the crown is in a conformation that is identical to that observed in unbound receptors **2** and **3** (29, 30). The key features are that the crown is in a "parallelogram" conformation and the sidearms point in opposite directions from the macrocycle.

The repulsive nature of the fluorinated aromatic ring toward K^+ can be seen clearly in the crystal structure of **4**·KI (Fig. 1 *d* and *e*). The solid state structure of **4**·KI revealed no sidearm coordination of the ring-bound K^+ ion. Both top and side views of the solid state KI structures of **1** and **4** are shown in space-filling views in Fig. 1*e*. Despite the dramatic difference between **1** and **4**, the macrocyclic portion of the complex was essentially identical in both cases. Both crowns are in the D_{3d} conformation (Fig. 1*e*). The K^+ to oxygen distances are 2.68 ± 0.05 Å for **1**·K^+ and 2.78 ± 0.05 Å for **4**·KI. Likewise, the K^+ to nitrogen distances were similar: 3.06 Å and 3.01 Å. The sidearms of **1**·K^+ are turned inward toward the center of the macroring to maximize cation contact. The sidearms are in the *anti* conformation rather than on the same side (*syn*) of the macroring. Owing to the difference in sidearm donicity, the sidearm conformations are *gauche* (58.8°) in **1**·K^+ (*anti* sidearms) and *antiperiplanar* (176.5°) in **4**·K^+ (sidearms extended from the macroring). Because K^+ is not involved in π complexation in the fluorinated receptor, **4**, it is coordinated by the I^- counterion (Fig. 1*e*).

Conclusion and Significance for Biology. The ability to design and evaluate in detail low-molecular weight model systems provides a powerful tool for studying cation-π interactions. The evidence presented here and the body of data that exists on alkali metal cation-π interactions clearly indicate that biological systems also may use aromatic groups to bind cations. The lack of documentation of alkali metal cation-π interactions in biology may be attributed to at least two factors. First, the resolution of many structures is not sufficient for the unequivocal assignment of electron density as Na^+, K^+, or $(H_2)O$. In fact, Na^+ and H_2O have the same number of electrons, and the scattering factors of all three species are similar. Methods have been developed for the screening of potential Na^+ binding sites in proteins, but the procedure relies on the presence of typical σ coordination environments (35). Second, even when resolution is sufficient, the interaction between a cation and an aromatic side chain simply may be overlooked by the crystallographer because such interactions are not yet well known. During the course of refining a structure, electron density may be assigned as a water molecule even though the chemical environment suggests the presence of a Na^+ or K^+ cation (for example, see Fig. 2).

A survey of several structures in the Protein Data Bank revealed a few cases in which a putative water molecule was located near an aromatic ring. One intriguing example was found in a 2.1-Å resolution structure of the enzyme tryptophanase (PDB ID code 1AX4) (36). In this enzyme, a putative water (H_2O 374, atom number 15153) is located 3.7 Å from the centroid of the aromatic ring of Tyr429. This value is close to the K^+-centroid distances that we observed in the synthetic receptors (3.43–3.45 Å). The "water" is also in close contact (2.6 Å) with the carbonyl oxygen of Tyr429. From a search of the CSD, we were able to determine the typical distances for a water molecule hydrogen-bonded to the carbonyl oxygen of a secondary amide. The average O_{water}-$O_{carbonyl}$ distance (obtained from the CSD) was 3.10 ± 0.36 Å. Interestingly, similar CSD searches for Na^+-$O_{carbonyl}$ (2.49 ± 0.35 Å) or K^+-$O_{carbonyl}$ (2.85 ± 0.38 Å) interactions more closely match the distance of 2.6 Å in the tryptophanase example. Experienced crystallographers determined the tryptophanase structure and the assignment of H_2O 374 could well be correct. However, given its position over the face of the aromatic ring, the observed distances, and the similarity in scattering factors for Na^+, K^+, and O, we propose that it is an alkali metal cation.

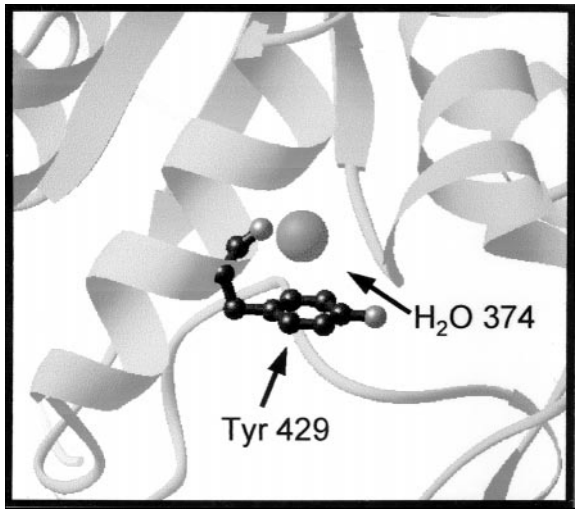

Fig. 2. Water molecule assigned in the crystal structure of tryptophanase (PDB ID code 1AX4). Fig. 2 was created with RIBBONS Version 2.63 (37).

The results presented here confirm that arenes can serve as π donors for alkali metal cations. We anticipate that as the resolution and number of protein crystal structures increase, more examples will be found of alkali metal cation-π interactions involving the aromatic amino acid side chains. The consequences of this type of binding site for protein function can begin to be assessed as more examples are found and subsequent mutagenesis studies are performed. Finally, we hope that the results of the studies presented here will stimulate a consideration of cation-π interactions in cases where only water has previously been inferred.

We thank the National Institutes of Health (GM-36262) and the National Science Foundation (CHE-9805840) for grants that supported this work. We are also grateful for an American Chemical Society Division of Organic Chemistry fellowship, funded by Procter & Gamble, to E.S.M. We appreciate helpful discussions with Professor F. Scott Mathews.

1. Suelter, C. H. (1970) *Science* **168,** 789–795.
2. Black, C. B., Huang, H.-W. & Cowan, J. A. (1994) *Coord. Chem. Rev.* **135,** 165–202.
3. Woehl, E. U. & Dunn, M. F. (1995) *Coord. Chem. Rev.* **144,** 147–197.
4. Toney, M. D., Hohenester, E., Cowan, S. W. & Jansonius, J. N. (1993) *Science* **261,** 756–759.
5. Di Cera, E., Guinto, E. R., Vindigni, A., Dang, Q. D., Ayala, Y. M., Wuyl, M. & Tulinsky, A. (1995) *J. Biol. Chem.* **279,** 22089–22092.
6. Larsen, T. M., Laughlin, L. T., Holden, H. M., Rayment, I. & Reed, G. H. (1994) *Biochemistry* **33,** 6301–6309.
7. Wilbanks, S. M. & McKay, D. B. (1995) *J. Biol. Chem.* **270,** 2251–2257.
8. Villeret, V., Huang, S., Fromm, H. J. & Lipscomb, W. N. (1995) *Proc. Natl. Acad. Sci. USA* **92,** 8916–8920.
9. Yamashita, M. M., Wesson, L., Eisenman, G. & Eisenberg, D. (1990) *Proc. Natl. Acad. Sci. USA* **87,** 5648–5652.
10. Mecozzi, S., West, A. P., Jr., & Dougherty, D. A. (1996) *J. Am. Chem. Soc.* **118,** 2307–2308.

11. Dunbar, R. C. (1998) *J. Phys. Chem. A* **102,** 8946–8952.
12. Cubero, E., Luque, F. J. & Orozco, M. (1998) *Proc. Natl. Acad. Sci. USA* **95,** 5976–5980.
13. Sunner, J., Nishizawa, K. & Kebarle, P. (1981) *J. Phys. Chem.* **85,** 1814–1820.
14. Guo, B. C., Purnell, J. W. & Castleman, A. W., Jr. (1990) *Chem. Phys. Lett.* **168,** 155–160.
15. Cabarcos, O. M., Weinheimer, C. J. & Lisy, J. M. (1998) *J. Chem. Phys.* **108,** 5151–5154.
16. Atwood, J. L. (1985) *J. Incl. Phenom.* **3,** 13–20.
17. Beer, P. D., Drew, M. G. B., Gale, P. A., Leeson, P. B. & Ogden, M. I. (1994) *J. Chem. Soc. Dalton Trans.* **23,** 3479–3485.
18. King, B. T., Noll, B. C. & Michl, J. (1999) *Collect. Czech. Chem. Commun.* **64,** 1001–1012.
19. Ma, J. C. & Dougherty, D. A. (1997) *Chem. Rev. (Washington, DC)* **97,** 1303–1324.
20. Kooystra, P. J. U., Kalk, K. H. & Hol, W. G. J. (1988) *Eur. J. Biochem.* **177,** 345–349.
21. Liaw, S.-H., Kuo, I. & Eisenberg, D. (1995) *Protein Sci.* **4,** 2358–2365.
22. Labesse, G., Ferrari, D., Chen, Z.-w., Rossi, G.-L., Kuusk, V., McIntire, W. S. & Mathews, F. S (1998) *J. Biol. Chem.* **273,** 25703–25712.
23. Wouters, J (1998) *Protein Sci.* **7,** 2472–2475.
24. McFail-Isom, L., Shui, X. & Williams, L. D. (1998) *Biochemistry* **37,** 17105–17111.
25. Scrutton, N. S. & Raine, A. R. C. (1996) *Biochem. J.* **319,** 1–8.
26. Burley, S. K. & Petsko, G. A. (1986) *FEBS Lett.* **203,** 139–143.
27. Gallivan, J. P. & Dougherty, D. A. (1999) *Proc. Natl. Acad. Sci. USA* **96,** 9459–9464.
28. Gokel, G. W. & Schall, O. F. (1996) in *Comprehensive Supramolecular Chemistry*, ed. Gokel, G. W (Pergamon, Oxford), pp. 97–152.
29. De Wall, S. L., Barbour, L. J. & Gokel, G. W. (1999) *J. Am. Chem. Soc.* **121,** 8405–8406.
30. De Wall, S. L., Meadows, E. S., Barbour, L. J. & Gokel, G. W. (1999) *J. Am. Chem. Soc.* **121,** 5613–5614.
31. Blessing, R. H (1995) *Acta Crystallogr. A* **51,** 33–38.
32. Gatto, V. J. & Gokel, G. W. (1984) *J. Am. Chem. Soc.* **106,** 8240–8244.
33. Shannon, R. D. (1976) *Acta Crystallogr. A* **32,** 751–767.
34. Gandour, R. D., Fronczek, F. R., Gatto, V. J., Minganti, C., Schultz, R. A., White, B. D., Arnold, K. A., Mazzocchi, D., Miller, S. R. & Gokel, G. W. (1986) *J. Am. Chem. Soc.* **108,** 4078–4088.
35. Nayal, M. & Di Cera, E. (1996) *J. Mol. Biol.* **256,** 228–234.
36. Isupov, M. N., Antson, A. A., Dodson, E. J., Dodson, G. G., Dementieva, I. S., Zakomirdina, L. N., Wilson, K. S., Dauter, Z., Lebedev, A. A. & Harutyunyan, E. H. (1998) *J. Mol. Biol.* **276,** 603–623.
37. Carson, M. (1997) *Methods Enzymol.* **277,** 493–505.